Level structure of ^{95}Nb

M. A. Rahman and M. S. Chowdhury
Department of Physics, University of Dhaka, Dhaka-1000, Bangladesh
(Received 11 January 2005; revised manuscript received 3 August 2005; published 14 November 2005)

The level structure of the ^{95}Nb nucleus has been studied with the (t, p) reaction in ^{93}Nb using a tandem Van de Graaff accelerator and a multichannel magnetic spectrograph at an incident beam energy of 12 MeV. Proton spectra are obtained at 12 different angles from 5° to 87.5° at an interval of 7.5°. Measurements of the proton distributions from the ^{93}Nb$(t, p)^{95}$Nb reaction were made for the ground and 54 excited states up to the excitation energy of 3.669 MeV. Absolute differential cross sections for the levels have been measured. The experimental angular distributions are compared with the theoretical distorted-wave Born approximation calculations to determine L values and J^π values. The level structure of ^{95}Nb is compared with previous results.

DOI: 10.1103/PhysRevC.72.054303 PACS number(s): 21.10.Hw, 24.10.Eq, 25.55.Hp, 27.60.+j

I. INTRODUCTION

The region of neutron-rich isotopes around $A = 100$ is of substantial interest because of the interplay between shell effect and the pairing force. The nuclear properties of the neutron-rich odd ^{95}Nb nucleus have been investigated with the (^{3}He,d), (d,^{3}He), $(\alpha, 2p)$, (α, t) and (t, α) reactions [1–5] and from the decay of ^{95}Zr [6]. The nuclei Sr, Zr, Mo, and Ru exist in the transitional region because of the transition in shapes from spherical to deformed [7–10]. This state of affairs should be reflected on the niobium nuclei because of their position near the center of the region of transition [5,11,12].

The study of the nuclear structure of these neutron-rich nuclei is being augmented from both the theoretical and experimental view points because they belong to a new region of deformation [13,14]. The nuclei in this region significantly change their shape from spherical to deformed as a function of increasing neutron number. The theoretical suggestions indicate that the tendency toward deformation in this region may be dominated by a strong isoscalar residual interaction between particles in the $1g_{9/2}$ proton orbital and the $1g_{7/2}$ neutron orbital [15,16]. Thus, these nuclei demonstrate a different characteristic feature from the adjacent nuclei. It is possible to investigate these with the aid of two-nucleon transfer reactions. These reactions exhibit a strong selectivity based on the degree to which the transferred nucleons are correlated in the final state [17]. The (t, p) reaction is more attractive than the other two-nucleon transfer reactions since two neutrons must be captured with $S = 0$. This reaction is a useful probe for examining the details of the nuclear structure from shell-model and pairing-multipole viewpoints. Neutron-rich nuclei not easily accessible through other reactions can be formed with this reaction.

Bhatt and Ball [18] calculated the level structure of the ^{95}Nb nucleus considering the residual interactions of protons in the $1g_{9/2}$ orbit and neutrons in the $2d_{5/2}$ orbit outside the semiclosed core of ^{90}Zr. In addition, Vervier [19] included particles in the $2p_{1/2}$ orbit, but their calculations were not beyond 2.00 MeV. Gloeckner [20] also calculated the level structure up to an excitation energy of 1.657 MeV by taking a ^{88}Sr core with protons filling the $(2p_{1/2}, 1g_{9/2})$ levels and neutrons the $(2d_{5/2}, 3s_{9/2})$ levels.

The review of the experimental and theoretical studies reveals that the attention paid to odd A niobium isotopes was much less than that given to the neighboring nuclei. In particular, no attempt had been made to investigate the nuclear properties of the ^{95}Nb nucleus using the (t, p) reaction. The angular distributions of the observed levels in the present experiment have been measured for a wider range of angles up to 87.5° and are analyzed by using the distorted-wave Born approximation (DWBA) calculations.

II. EXPERIMENTAL PROCEDURE

A beam of tritons from the tandem Van de Graaff accelerator at the Atomic Weapons Research Establishment (AWRE), Aldermaston, was used to bombard the ^{93}Nb target, and the reaction product protons were analyzed with a multichannel magnetic spectrograph in an 11.15 kG magnetic field [21]. The instrument permits the simultaneous recording of 24 energy spectra in the angular range 5° to 175°. The integrated beam current was 10 000 μC. The triton beam was focused as a rectangular spot 1.5 mm wide and 1.0 mm high on the target. Protons were detected by means of Ilford K2 emulsion plates 50 μm thick mounted in the focal plane of each channel.

The ^{93}Nb$(t, p)^{95}$Nb experiment was carried out at an incident triton beam energy of 12 MeV using a target approximately 250 μg/cm^2 thick. The target obtained from Oak Ridge National Laboratory was self-supporting and isotopically 100% enriched. The energy resolution of this reaction was ~15 keV (full width at half maximum). The measurement was made at 12 angles between 5° to 87.5°.

Polythene absorbers 0.25 mm thick were placed in front of the emulsion in the (t, p) experiment to stop particles other than protons and to improve the quality of the proton tracks. The emulsion plates were taken out from the spectrograph after completing the exposure and then were developed using the standard method [22]. The Q values were obtained from the input plate position of proton groups at four different angles (35°, 42.5°, 50°, and 65°) using a computer program. The excitation energy of a particular group was measured by subtracting the Q value of that group from the Q value of the ground state. The excitation energy quoted for each level is the

TABLE I. Triton and proton optical-model parameters used in the DWBA calculations.

Particle	V (MeV)	r_0 (fm)	a_0 (fm)	W (MeV)	r_1 (fm)	a_1 (fm)	V_s (MeV)	W_s (MeV	r_s (fm)	a_s (fm)
t	157.10	1.241	0.667	16.50	1.530	0.798	8.340	1.018	1.588	0.334
p	56.81	1.17	0.75	0.0	1.32	0.59	6.20	10.21	1.01	0.75

mean of the excitation energies at those angles. Absolute cross sections for the elastic triton data were obtained by normalizing the (t, t) angular distributions to the cross sections predicted by the optical-model calculation that produced the best fit to the experimental data. The cross section for the ground-state transition of the ^{93}Nb $(t, p)^{95}$Nb reaction was measured in a separate short exposure by recording the proton group in the bottom half of the plate as the elastically scattered triton group was being recorded on the top half of the plate of the ^{93}Nb $(t, t)^{93}$Nb exposure. The result was finally normalized to the ground-state count of the ^{93}Nb $(t, p)^{95}$Nb long exposure to obtain the absolute differential cross section for different levels in the ^{95}Nb nucleus.

III. DWBA ANALYSIS

Distorted-wave Born approximation (DWBA) calculations were carried out using the computer code DWUCK4 [23]. The optical model potential was of the form

$$U(r) = V_c(r) - V(1+e^x)^{-1} + 4iw\, d/dx'(1+e^{x'})^{-1} + (\hbar/m_\pi c)^2 r^{-1}(V_{so} + iW_{so})x d/dr(1+e^{x_s})^{-1}\sigma\cdot 1,$$

where $x = (r - r_0A^{1/3})/a_0$, $x' = (r - r_1A^{1/3})/a_1$, $x_s = (r - r_sA^{1/3})/a_s$, and σ is spin of the incident particle. The Coulomb potential $V_c(r)$ is due to a uniformly charged spherical nucleus of radius $R_c = r_cA^{1/3}$ and charge Z. The Coulomb radius was 1.3 $A^{1/3}$ fm. V and W are the depths of the real and imaginary potential wells, $r_0A^{1/3}$ is the mean radius of the well, and a is a measure of surface diffuseness. Optical-model parameters summarized in Table I were obtained from the analysis of elastic scattering of tritons [24] and protons [25].

The DWBA program was run for different L transitions with $0 \leqslant L \leqslant 5$ for the levels in the energy range 0.000–3.669 MeV. The L value of each transition was determined on the closeness of the DWBA fit to the experimental points. The angular distributions corresponding to an L value transfer of 0 are forward peaked with a secondary maximum around 32.5°. The angular distributions for $L = 1, 2, 3, 4$, and 5 transfers are peaked at 12.5°, 20°, 30°, 37.5°, and 47.5°, respectively.

IV. RESULTS AND DISCUSSION

The energy level spectra for the ^{95}Nb nucleus have been obtained from the ^{93}Nb $(t, p)^{95}$Nb reaction. Energies of the 55 levels (0.000–3.669 MeV) with their uncertainties are presented in Table II. This table also contains values of L transfers, J^π, and previous results. A typical proton energy spectrum measured at an angle of 50° to the incident beam direction is shown in Fig. 1. The mean ground-state Q value was found to be 7.897 ± 0.012 MeV. The angular distributions are shown in Fig. 2, where smooth curves represent the prediction of DWBA calculations. The angular momentum L has been assigned by comparing the shape of the experimental angular distribution with the calculated one. The agreements between the measured angular distributions and theoretical predictions are satisfactory, and the L values and parities of 50 levels have been assigned unambiguously.

The initial spin and parity of the target nucleus ^{93}Nb are known to be 9/2$^+$. In the (t, p) reaction, the L value of the transferred particles plays a vital role in determining the spin and parity of the state of the residual nucleus as the two identical particles must be in a spin of antisymmetric state ($S = 0$). The $L = 0$ transfer can populate only a 9/2$^+$ state in ^{95}Nb. In principle, $L = 1, 2, 3$, and 4 transfers can populate states with $J^\pi = (7/2 \rightarrow 11/2)^-$, $(5/2 \rightarrow 13/2)^+$, $(3/2 \rightarrow 15/2)^-$ and $(1/2 \rightarrow 17/2)^+$, respectively.

The following levels in the excitation energy region up to 3.669 MeV are observed to exhibit an angular distribution characteristic of $L = 0$ transfer: 1.088, 1.268, 1.337, 1.565, 1.658, 1.903, 1.958, 2.018, 2.637, 2.765, 2.947, 3.111, 3.149, 3.196, 3.307, and 3.358 MeV. Since the ground state of ^{93}Nb is 9/2$^+$, these $L = 0$ transitions uniquely identify the above levels as 9/2$^+$.

0.805 MeV level. The 0.805 MeV level populated in the present work is assigned J^π =$(5/2 \rightarrow 13/2)^+$. The J^π value of the level at 799.5 keV was reported as 3/2$^-$ in NDS [26], which does not agree with the observed values.

1.088 and 1.268 MeV levels. These levels are assigned the definite J^π value of 9/2$^+$. The level at 1088 keV from the ^{97}Mo$(d, a)^{95}$Nb reaction was reported in NDS [26] without any spin assignment. The level at 1273.8 keV reported in NDS [26] was assigned 5/2$^-$, which is not in agreement with the present value.

1.518 MeV level. The level at 1514 keV reported in NDS [26] was not assigned a spin value. This level is assigned $J^\pi = (5/2 \rightarrow 13/2)^+$ in the present work.

1.658 and 1.903 MeV levels. The transitions to these levels exhibit angular distributions with $L = 0$ shapes, and they are assigned the definite spin value of 9/2$^+$. The levels at 1662.8 and 1903.10 keV from the (t, α) reaction reported in NDS [26] were assigned $J^\pi = (5/2^-)$ and $J^\pi = 3/2^+, 5/2^+$, respectively.

2.052 and 2.165 MeV levels. The predictions of $L = 3$ transfer fit the angular distributions of 2.052 and 2.165 MeV levels. Flynn *et al.* [5] identified these levels, but their assignments $J^\pi = 3/2^+, 5/2^+$ are not in agreement with our values $J^\pi = (3/2 \rightarrow 15/2)^-$.

2.305, 2.362, and 2.390 MeV levels. In the present experiment, we observed these levels, and their angular distributions

TABLE II. Results of the ^{93}Nb$(t, p)^{95}$Nb reaction and Previous results.

Group no.	Present experiment			Previous results [26]	
	Energy (MeV)	L	J^{π}	Energy (keV)	J^{π}
0	0.000	0	$9/2^{+}$	0	$9/2^{+}$
1	0.260 ± 0.005			235.68	$1/2^{-}$
				724.202	$7/2^{+}$
				730.6	$(5/2)^{+}$
2	0.767 ± 0.007	2	$(5/2 \rightarrow 13/2)^{+}$	756.732	$7/2^{+}$
3	0.805 ± 0.005	2	$(5/2 \rightarrow 13/2)^{+}$	799.5	$3/2^{-}$
4	0.877 ± 0.007	2	$(5/2 \rightarrow 13/2)^{+}$		
5	1.009 ± 0.010			1011.8	$(5/2)^{-}$
6	1.088 ± 0.011	0	$9/2^{+}$	1088	
7	1.149 ± 0.011	2	$(5/2 \rightarrow 13/2)^{+}$		
8	1.216 ± 0.007	1	$(7/2 \rightarrow 11/2)^{-}$	1219.6	$3/2^{-}$
9	1.268 ± 0.007	0	$9/2^{+}$	1273.8	$5/2^{-}$
10	1.337 ± 0.009	0	$9/2^{+}$		
				1364.8	
11	1.394 ± 0.009				
				1430.12	$(3/2^{+})$
12	1.464 ± 0.005				
13	1.518 ± 0.008	2	$(5/2 \rightarrow 13/2)^{+}$	1514	
14	1.565 ± 0.008	0	$9/2^{+}$		
				1589.8	$3/2^{-}$
				1590.8	$3/2^{+}, 5/2^{+}$
15	1.616 ± 0.008	4	$(1/2 \rightarrow 17/2)^{+}$	1623.12	$3/2^{+}, 5/2^{+}$
				1645.8	$1/2^{-}, 3/2^{-}$
16	1.658 ± 0.008	0	$9/2^{+}$	1662.8	$(5/2)^{-}$
				1710.10	$(7/2^{+})$
17	1.730 ± 0.007	2	$(5/2 \rightarrow 13/2)^{+}$		
18	1.767 ± 0.004	1	$(7/2 \rightarrow 11/2)^{-}$		
				1813.6	$5/2^{+}$
19	1.847 ± 0.002	2	$(5/2 \rightarrow 13/2)^{+}$		
20	1.903 ± 0.015	0	$9/2^{+}$	1903.10	$3/2^{+}, 5/2^{+}$
21	1.958 ± 0.009	0	$9/2^{+}$	1972.8	-
22	2.018 ± 0.016	0	$9/2^{+}$		
23	2.052 ± 0.006	3	$(3/2 \rightarrow 15/2)^{-}$	2058.10	$3/2^{+}, 5/2^{+}$
24	2.100 ± 0.009				
				2135.14	$3/2^{+}, 5/2^{+}$
25	2.165 ± 0.011	3	$(3/2 \rightarrow 15/2)^{-}$	2172.8	$3/2^{+}, 5/2^{+}$
26	2.200 ± 0.005	2	$(5/2 \rightarrow 13/2)^{+}$		
27	2.275 ± 0.014	4	$(1/2 \rightarrow 17/2)^{+}$		
28	2.305 ± 0.014	2	$(5/2 \rightarrow 13/2)^{+}$	2302.8	$5/2^{-}$
				2328.12	$1/2^{-}, 3/2^{-}$
29	2.362 ± 0.004	2	$(5/2 \rightarrow 13/2)^{+}$	2373.8	$(1/2^{+})$
30	2.390 ± 0.007	2	$(5/2 \rightarrow 13/2)^{+}$	2383.8	$1/2^{-}$
				2414.8	$(3/2^{+})$
31	2.435 ± 0.006	2	$(5/2 \rightarrow 13/2)^{+}$	2431.8	$(3/2^{+}, 5/2^{+})$
32	2.486 ± 0.007	3	$(3/2 \rightarrow 15/2)^{-}$	2481.12	$5/2^{-}, 7/2^{-}$
33	2.536 ± 0.004	2	$(5/2 \rightarrow 13/2)^{+}$	2540.20	
34	2.586 ± 0.002	4	$(1/2 \rightarrow 17/2)^{+}$	2599.8	$5/2^{-}$
35	2.637 ± 0.004	0	$9/2^{+}$	2632.8	$(3/2^{+})$
				2670.8	$(5/2^{-})$
36	2.706 ± 0.002	2	$(5/2 \rightarrow 13/2)^{+}$		
				2724.8	$5/2^{-}$
37	2.765 ± 0.004	0	$9/2^{+}$	2768.8	$3/2^{-}$
				2786.15	$5/2^{-}, 7/2^{-}$
38	2.817 ± 0.006	3	$(3/2 \rightarrow 15/2)^{-}$	2815.8	
39	2.888 ± 0.006	2	$(5/2 \rightarrow 13/2)^{+}$	2896.8	

TABLE II. *(Continued.)*

Group no.	Present experiment			Previous results [26]	
	Energy (MeV)	L	J^{π}	Energy (keV)	J^{π}
40	2.947 ± 0.006	0	$9/2^+$	2977.10 3039.8	$3/2^+, 5/2^+$
41	2.993 ± 0.005	4	$(1/2 \rightarrow 17/2)^+$		
42	3.045 ± 0.007	3	$(3/2 \rightarrow 15/2)^-$		
43	3.111 ± 0.010	0	$9/2^+$	3110.20	
44	3.149 ± 0.003	0	$9/2^+$		
45	3.196 ± 0.015	0	$9/2^+$		
46	3.233 ± 0.009	4	$(1/2 \rightarrow 17/2)^+$		
47	3.307 ± 0.007	0	$9/2^+$		
48	3.358 ± 0.006	0	$9/2^+$		
49	3.408 ± 0.008	4	$(1/2 \rightarrow 17/2)^+$		
50	3.481 ± 0.007	4	$(1/2 \rightarrow 17/2)^+$	3510.20	
51	3.545 ± 0.003	4	$(1/2 \rightarrow 17/2)^+$		
52	3.585 ± 0.008	2	$(5/2 \rightarrow 13/2)^+$		
53	3.625 ± 0.005	4	$(1/2 \rightarrow 17/2)^+$		
54	3.669 ± 0.009	2	$(5/2 \rightarrow 13/2)^+$		

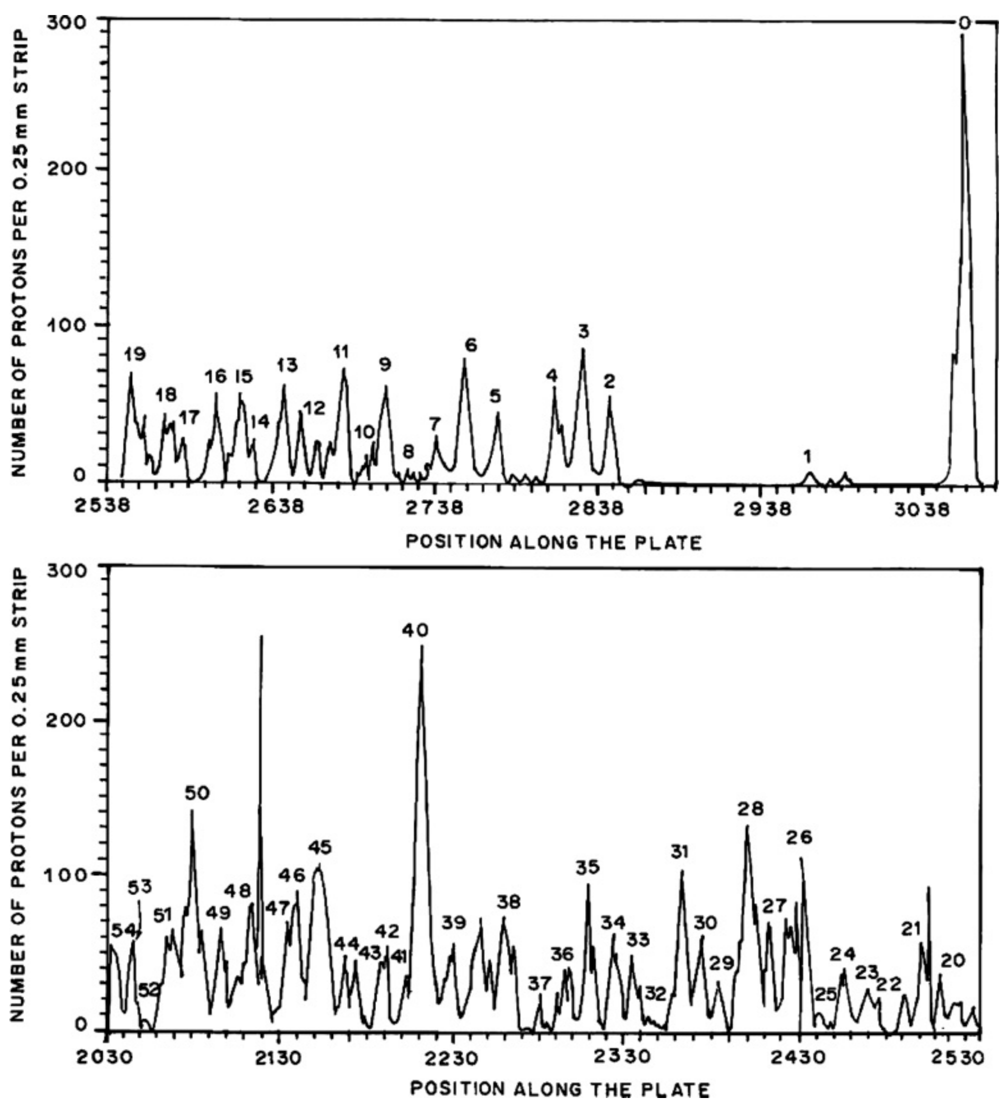

FIG. 1. Energy spectrum of protons emitted at 50° from the bombardment of ^{93}Nb with the 12 MeV triton.

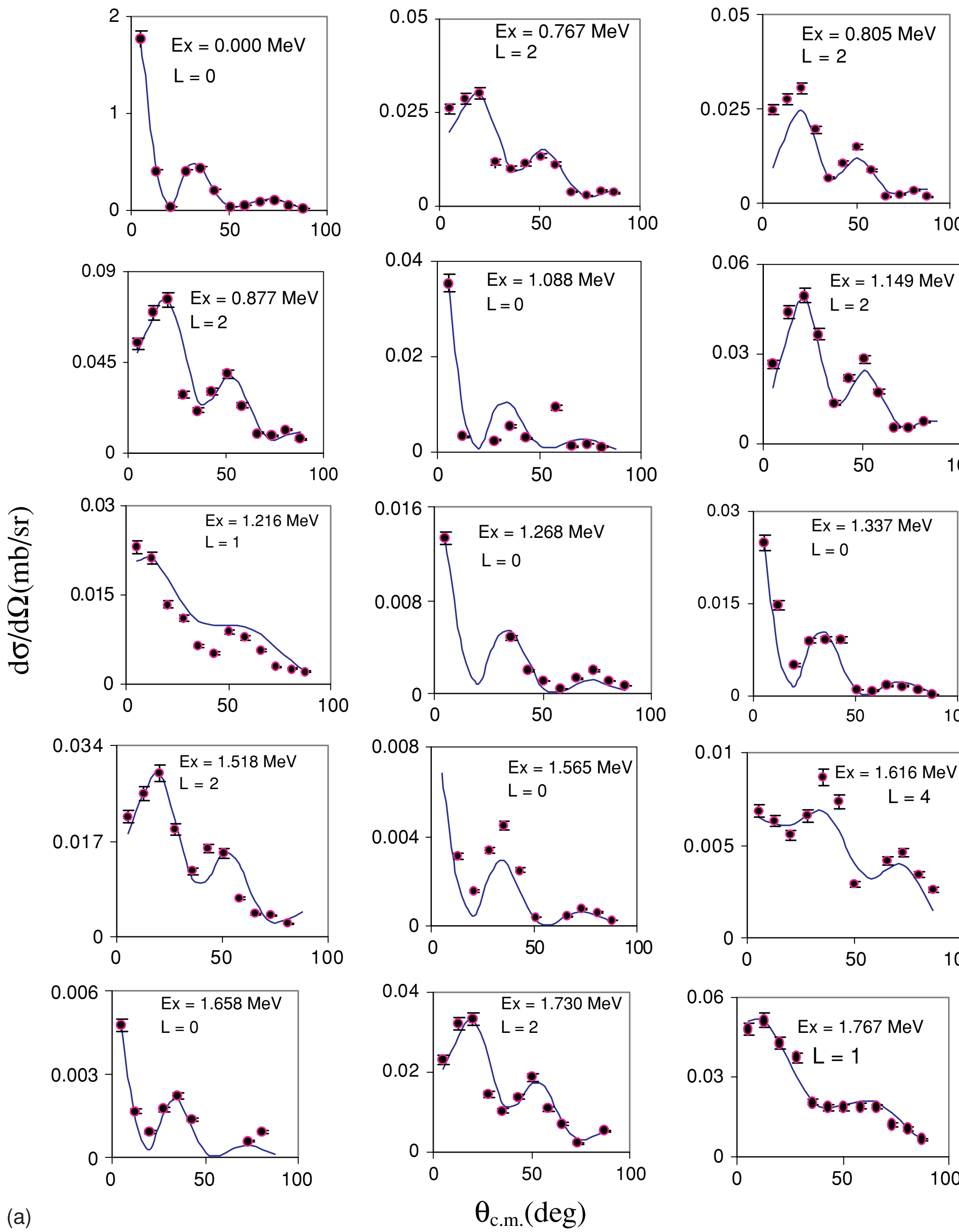

FIG. 2. (Color online) Angular distributions for the transitions to the ^{95}Nb levels whose excitation energy (MeV) and L transfer value are indicated. Experimental cross sections are shown as points with error bars. Solid lines are results of DWBA calculations.

are reproduced by $L = 2$ transfers, $J^{\pi} = (5/2 \rightarrow 13/2)^{+}$. Flynn *et al.* [5] assigned $5/2^{-}$ to a level at 2302.8 keV and $1/2^{-}$ to a level at 2383.8 keV, Zisman *et al.* [4] assigned doubtful $1/2^{+}$ to a level at 2373.8 keV.

2.586 MeV level. This level is assigned $J^{\pi} = (1/2 \rightarrow 17/2)^{+}$. The level at 2599.8 keV with spin $5/2^{-}$ from the (t, α) reaction was reported in NDS [26], which does not agree with the observed values.

2.637 and 2.765 MeV levels. These levels are assigned definite spin and parity values of $9/2^{+}$ due to $L = 0$ transfer. Flynn *et al.* [5] assigned doubtful $3/2^{+}$ to a level at 2632.8 keV and $3/2^{-}$ to a level at 2768.8 keV.

2.817, 2.888, and 3.111 MeV levels. The levels at 2815.8, 2896.8, and 3110.20 keV were reported from the (t, α) and $(^{3}\text{He},d)$ reactions in NDS [26] and the J^{π} values were not assigned to these levels. Our measured angular distributions for

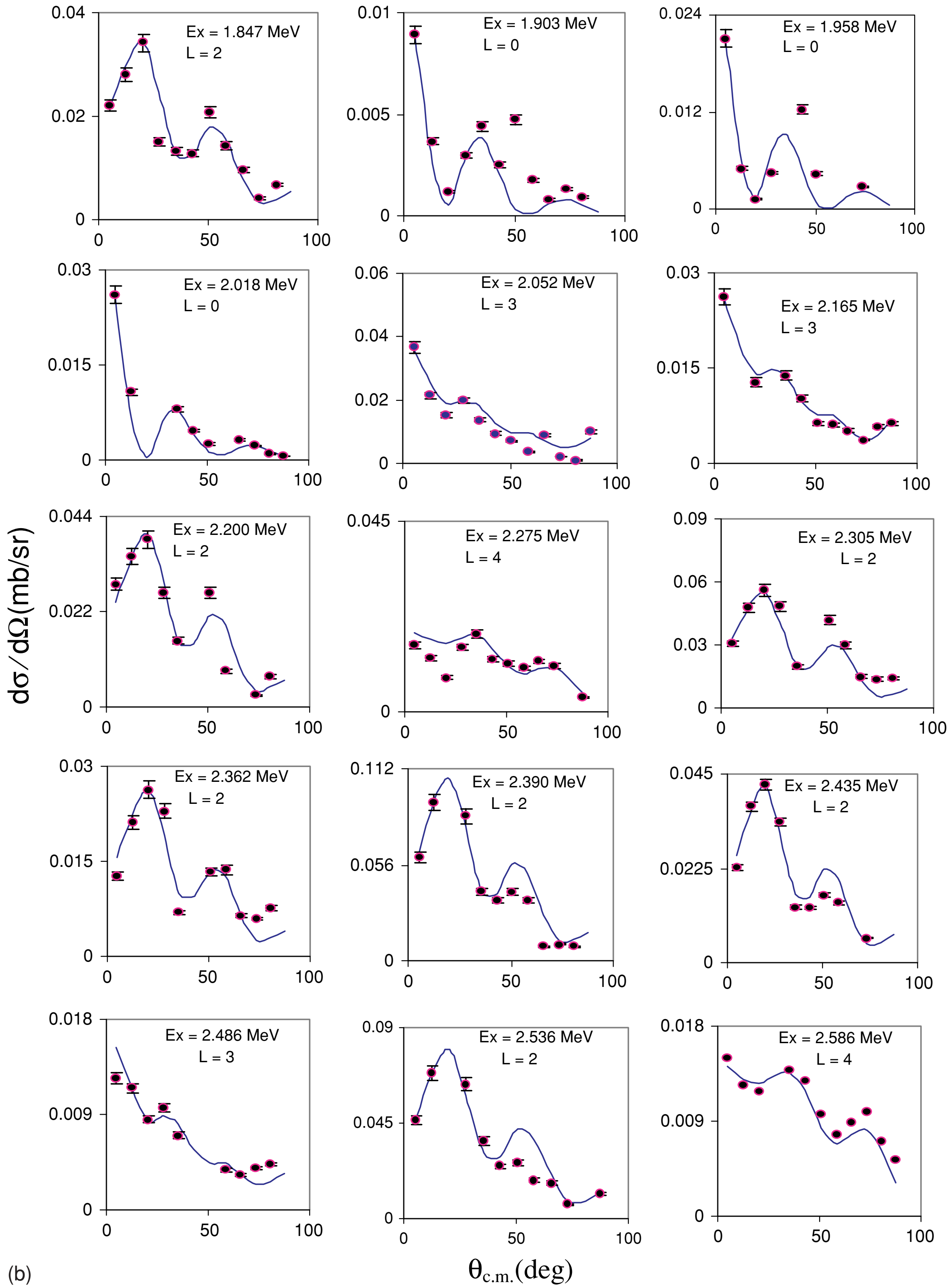

FIG. 2. (*Continued*.)

the levels at 2.817, 2.888, and 3.111 MeV are well reproduced by the $L = 3$, 2, and 0 transfers, respectively.

The angular distributions of the levels at 0.260, 1.009, 1.394, 1.464, and 2.100 MeV could not be shown because sufficient data could not be obtained at different angles due to emulsion disturbances. The levels at 1364.8 and 3510.2 keV reported in NDS [26], whose spin values have not been predicted, are not observed in the present work. These might be unnatural parity states because an unnatural parity state cannot be excited in the (t, p) reaction [27]. The large number

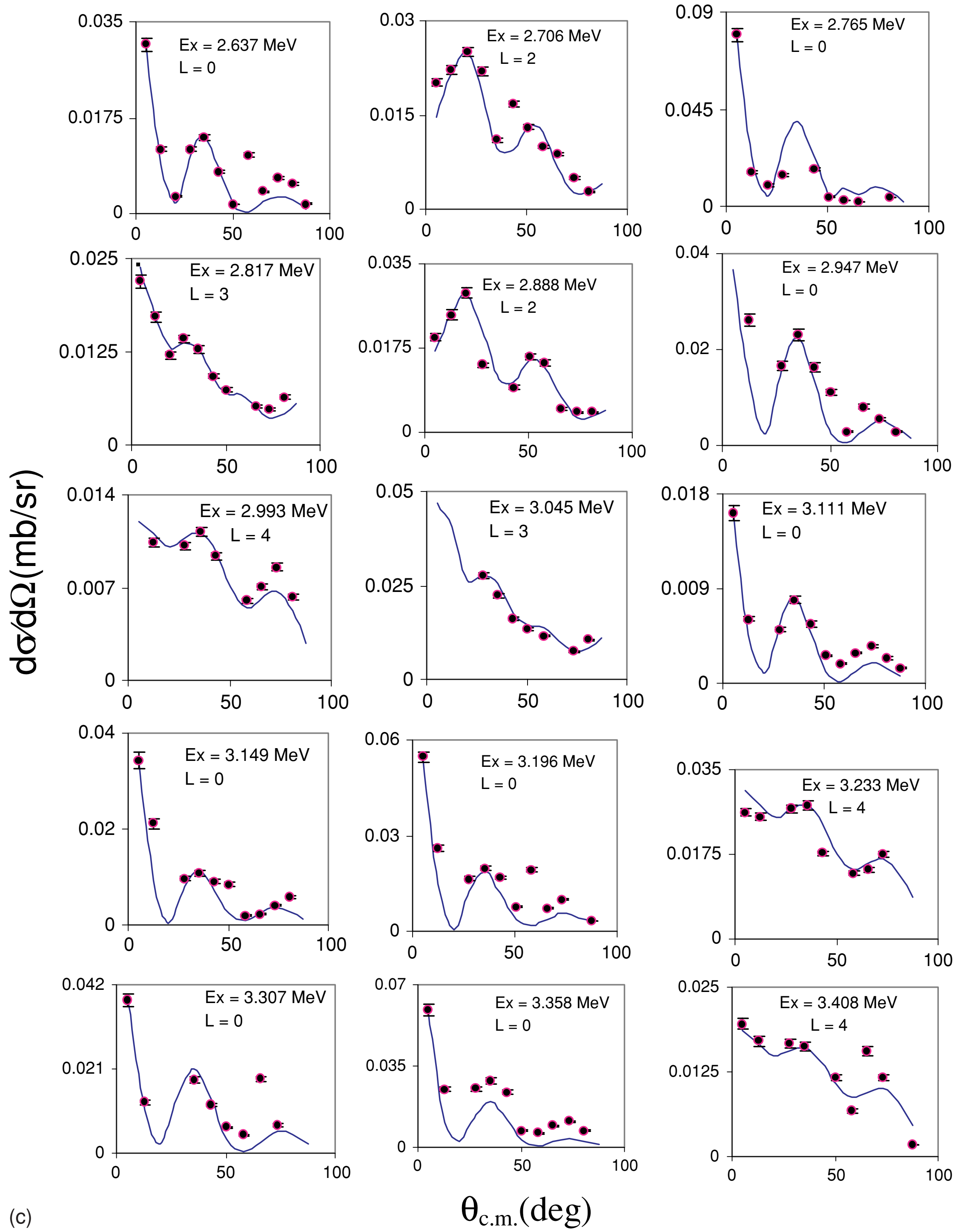

FIG. 2. (*Continued*.)

of states in the final nucleus are described by a single L transfer. This feature might be due to a particle vibration weak coupling structure, where the transfer in the odd-mass nucleus is characteristic of the transfer to the corresponding vibration in the even-even core [28].

The experimental level scheme obtained in the present investigation is shown in Fig. 3 together with the theoretical level schemes of ^{95}Nb calculated by assuming proton occupation of the $p_{1/2}$ and $g_{9/2}$ orbitals with a ^{88}Sr closed core [19,20]. As seen in this figure, the experimental levels are not well reproduced by the calculations. There is general agreement on the spin of the ground state. The levels at 0.767, 0.805, and 0.877 MeV are assigned $J^{\pi} = (5/2 \rightarrow 13/2)^{+}$ values in the present work. Gloeckner [20] predicted the levels at 0.756,

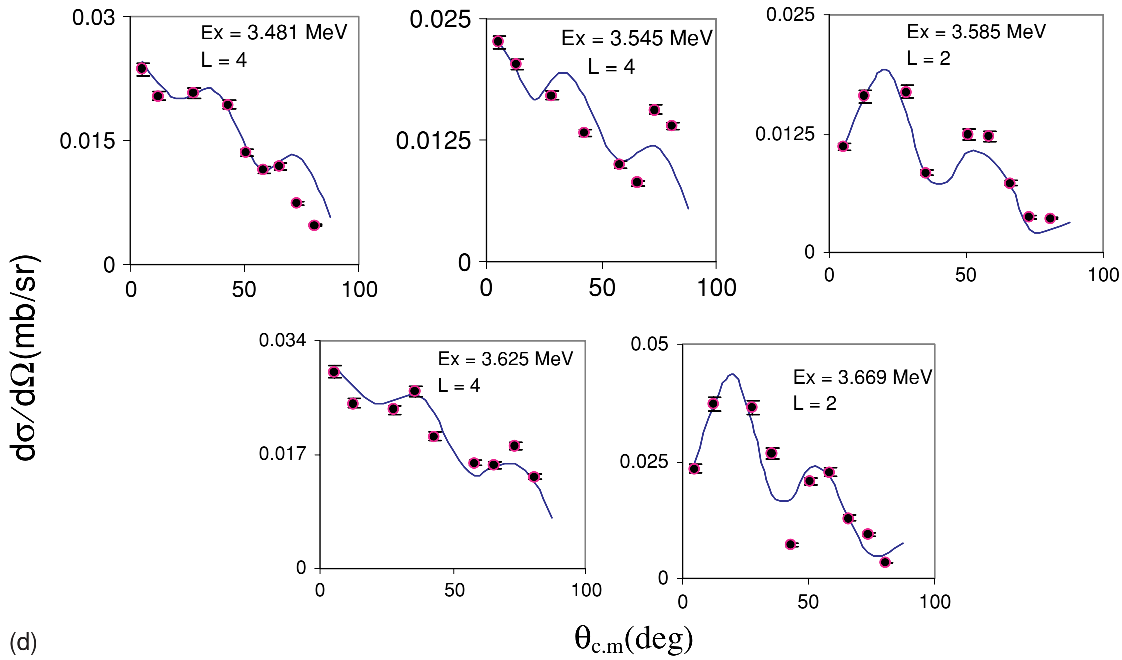

FIG. 2. (*Continued*.)

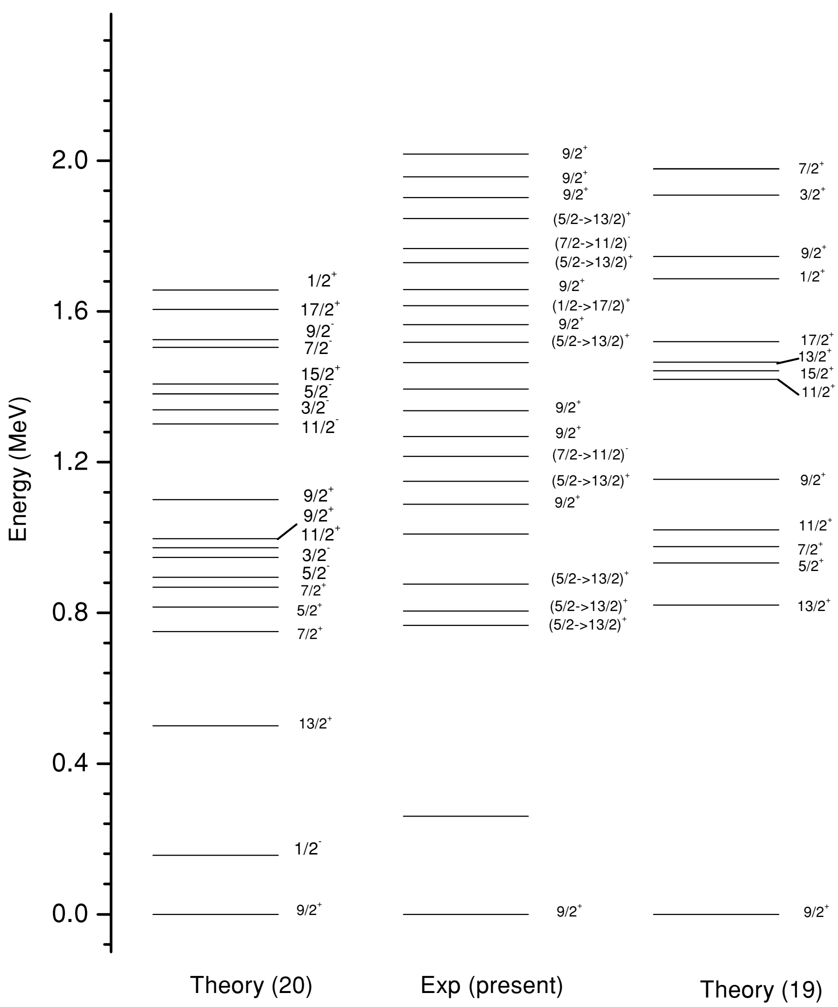

FIG. 3. Comparison of level scheme of ^{95}Nb as evinced in this investigation with theoretical level schemes [19,20].

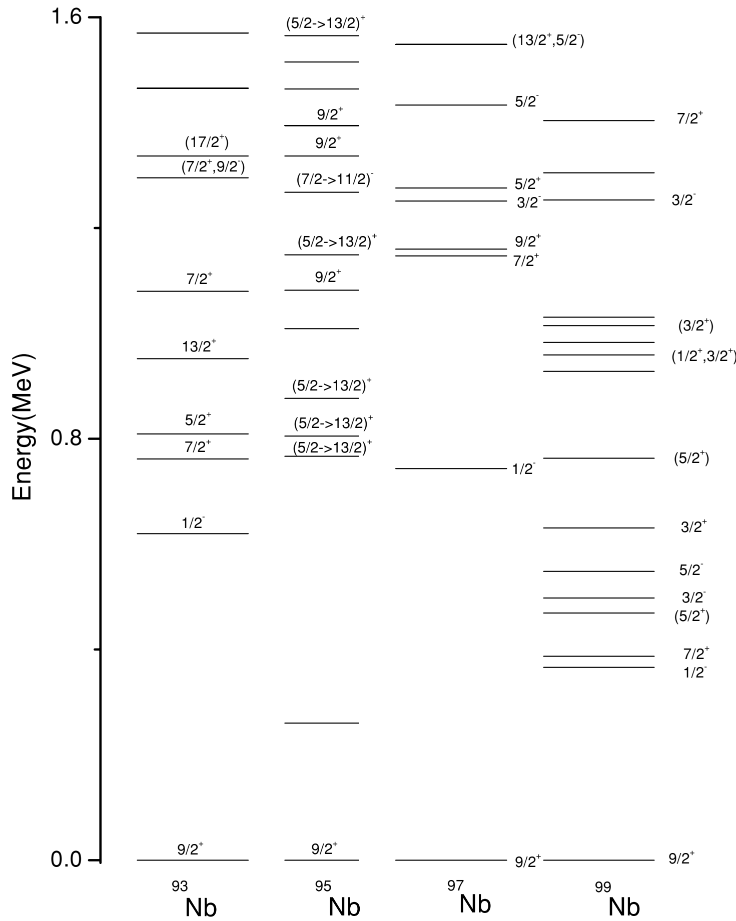

FIG. 4. Low-lying level schemes in odd Nb isotopes.

0.815, and 0.868 MeV with $J^\pi = 7/2^+$, $5/2^+$, and $7/2^+$, respectively, which agree with the current J^π values within the

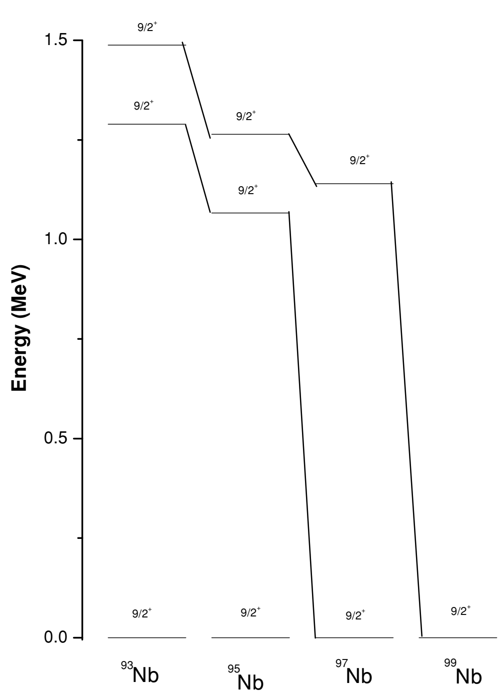

FIG. 5. Systematic lowering of $9/2^+$states in odd Nb isotopes.

range. The level at 1.088 MeV is assigned $9/2^+$ in this work. Gloeckner [20] predicted the $9/2^+$ value to a level at 1.100 MeV. The prediction of the $17/2^+$ assignment to a level at 1.606 MeV agrees with our observed $J^\pi = (1/2 \rightarrow 17/2)^+$ at 1.616 MeV. The even-even Zr and Mo nuclei form a smooth progression from symmetric rotor to vibrational structure if one considers the ground-state band in ^{102}Zr and ^{104}Mo together with the first excited 0^+bands in the progressively lighter Zr and Mo nuclei, respectively [27,29]. Coexistence of spherical and deformed properties plays a vital role in these isotopes. Strong mixing between these coexisting states might be expected to occur at low excitation energies, leading to large perturbation in the level density, level energies, and decay properties. A similar picture could also be valid in the Nb nuclei as they lie with the Zr, Mo nuclei in the same region. In Fig. 4, we show the level scheme obtained in the present experiment with the level schemes of ^{93,97,99}Nbnuclei in the low-lying region [4,5]. It is seen that compression in the energy levels occurs suddenly in ^{99}Nb, which may be an indication of a tendency toward deformation. It is worth examining the systematics of the low-lying $9/2^+$states among the four odd Nb isotopes. This is shown in Fig. 5, where the states of these spins are plotted with the neutron number. The $9/2^+$ states show the systematic trend toward lowering energies as a function of increasing neutron number. This characteristic feature indicates that ^{95}Nb exists in the transitional region. The shape transition from spherical to deformed occurs gradually

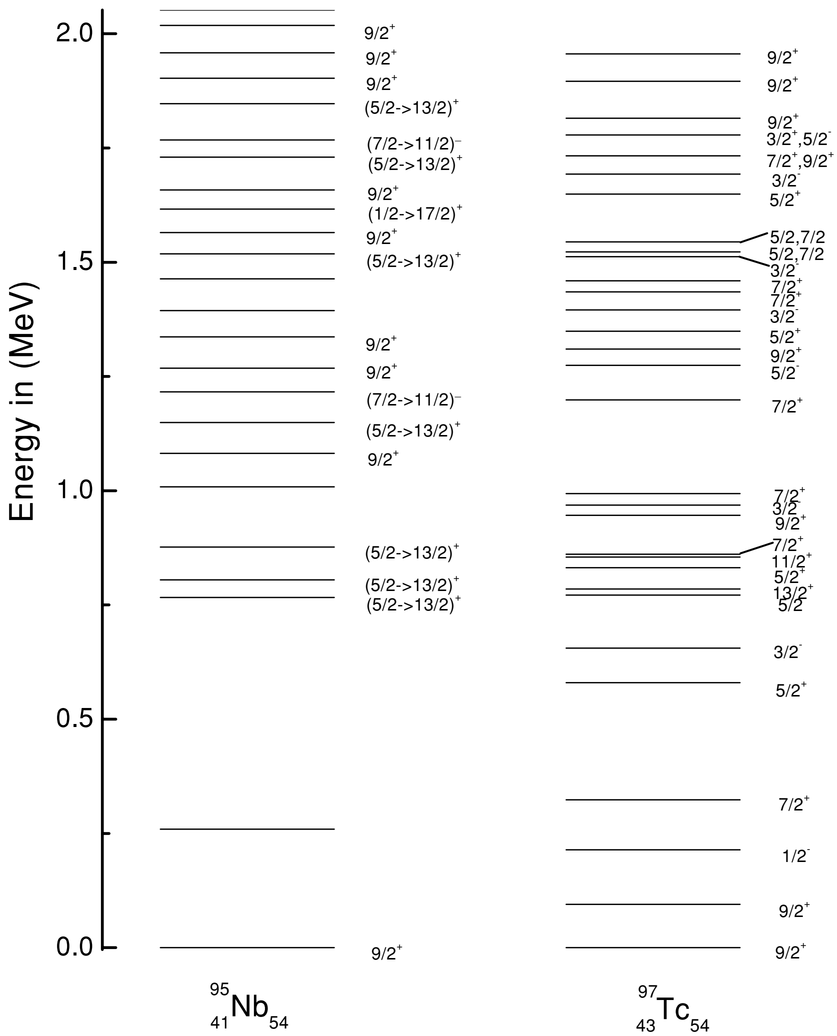

FIG. 6. Comparison of structure of $N = 54$ isotones.

as Z increases [10]. The Mo isotopes show rapid transition in shapes as a function of increasing neutron number [8,30]. The tendency of deformation was even more noticeable in the Tc isotopes [31]. It is useful to compare the structure of ^{95}Nb with the structure of its isotone $^{97}_{43}Tc_{54}$.

V. COMPARISON WITH THE LEVEL STRUCTURE OF $^{97}_{43}Tc_{54}$

An attempt has been made in Fig. 6 to compare the level scheme of the odd-mass $^{95}_{41}Nb_{54}$obtained in the present investigation with that of its isotone $^{97}_{43}Tc_{54}$.The data on ^{97}Tc have been taken from Kajrys *et al*. [32]. Both nuclei have the same ground-state spin and parity, 9/2$^+$. The 9/2$^+$ spin of the ground state in ^{95}Nb is explained by the shell model which predicts that the 13 protons outside the 28 protons magic shell fill up the $2p_{3/2}$, $1f_{5/2}$, $2p_{1/2}$, and $1g_{9/2}$ shells. Hence, the ground state of ^{95}Nb shows a proton configuration $(2p_{1/2})^2$, $(1g_{9/2})^1$. If more protons are added, the shell model predicts that protons start filling the $1g_{9/2}$ shell up to its capability. A similar situation exists in ^{97}Tc, where the ground-state configuration is $2p^2_{1/2}$, $1g^3_{9/2}$. There are two excited states in both nuclei at 1.903 and 1.958 MeV, which display spins of 9/2$^+$. The energy levels in ^{97}Tc are closely spaced, and the first and second excited 9/2$^+$states lie at much lower energy levels than those in ^{95}Nb. In addition, the first negative parity state occurs at a much higher energy in ^{95}Nb than it does in ^{97}Tc. The observed level scheme of ^{95}Nb seems to exhibit the tendency of deviation of shapes from sphericity.

VI. CONCLUSION

The level structure of ^{95}Nb has been studied up to 3.669 MeV with the $^{93}Nb(t, p)^{95}Nb$ reaction. A number of new energy levels have been found, and spin assignments were made for many of them. These results clearly indicate the effectiveness of the (t, p) reaction in populating the states. The systematics in energy of 9/2$^+$ states in Fig. 5 indicates that the ^{95}Nb nucleus may belong to the transitional region that exists near $A = 100$. The experimental levels are not well reproduced by the theoretical investigations. The attention given to the odd niobium nuclei either theoretically or experimentally is much less than that given to the nuclei in the region near $A = 100$. It is desirable to perform more work on niobium nuclei with as many techniques as possible.

ACKNOWLEDGMENTS

The authors thank the operating staff of the tandem accelerator at AWRE, Aldermaston for their cooperation and Professor P. D. Kunz, University of Colorado, for sending the DWUCK4 program. The cooperation of Dr. Saiful Islam, Centre for Management Studies, European University, Munich, is gratefully acknowledged. MSC is also grateful to the University of Bradford for financial support and to Professor G. Brown, Dr. W. Booth, and Mr. S. M. Dalgleish, University of Bradford, England, for their help with the exposed plates. MAR gratefully acknowledges a research fellowship of Bose Centre for Advanced Study and Research, Dhaka University. They also thank the staff of IIT, University of Dhaka, for use of the computer facilities.

[1] L. R. Medsker and J. L. Yntema, Phys. Rev. C **7**, 440 (1973).
[2] P. K. Bindal, D. H. Youngblood, and R. L. Kozub, Phys. Rev. C **10**, 729 (1974).
[3] S. Mukherjee and N. L. Singh, J. Phys. G: Nucl. Part. Phys. **22**, 1455 (1996).
[4] M. S. Zisman and B. G. Harvey, Phys. Rev. C **5**, 1031 (1972).
[5] E. R. Flynn, R. E. Brown, F. Ajzenberg-Selove, and J. A. Cizewski, Phys. Rev. C **28**, 575 (1983).
[6] S. M. Brahmaver and J. H. Hamilton, Phys. Rev. **187**, 1487 (1969).
[7] J. B. Gupta, J. Phys. G: Nucl. Part. Phys. **28**, 2365 (2003).
[8] J. M. Chatterjee, M. Saha-Sarkar, S. Bhattacharya, S. Sarkar, R. P. Singh, S. Murulithar, and R. K. Bhowmik, Phys. Rev. C **69**, 044303 (2004).
[9] J. Timar, J. Gizon, A. Gizon, D. Sohler, B. M. Nyako, L. Zolnai, A. J. Boston, D. T. Joss, E. S. Paul, A. T. Semple, C. M. Parryand, and I. Ragnarsson, Phys. Rev. C **62**, 044317 (2000).
[10] A. G. Smith *et al.*, Phys. Rev. Lett. **77**, 1711 (1996).
[11] G. Lhersonneau, S. Brant, and V. Paar, Phys. Rev. C **62**, 044304 (2000).
[12] J. K. Hwang *et al.*, J. Phys. G: Nucl. Part. Phys. **27**, L9 (2001).
[13] F. K. Wohn *et al.*, Phys. Rev. C **33**, 677 (1986).
[14] E. Cheifetz, R. C. Jared, S. G. Thompson, and J. B. Wilhelmy, Phys. Rev. Lett. **25**, 38 (1970).
[15] Ashok Kumar and M. R. Gunye, Phys. Rev. C **32**, 2116 (1985).
[16] P. Federman and S. Pittel, Phys. Lett. **B77**, 29 (1978).
[17] Norman K. Glendenning, Nucl. Phys. **29**, 109 (1962).
[18] K. H. Bhatt and J. B. Ball, Nucl. Phys. **63**, 286 (1965).
[19] J. Vervier, Nucl. Phys. **75**, 17 (1966).
[20] D. H. Gloeckner, Nucl. Phys. **A253**, 301 (1975).
[21] R. Middleton and S. Hinds, Nucl. Phys. **34**, 404 (1962).
[22] W. H. Barkas, Nuclear Research Emulsion, Part 1. Techniques and Theory (1963).
[23] P. D. Kunz, University of Colorado, unpublished.
[24] M. Shafi Chowdhury, Singapore Journal of Physics (submitted).
[25] F. D. Becchetti and G. W. Greenlees, Phys. Rev. **182**, 1190 (1969).
[26] T. W. Burrows, Nucl. Data Sheets **68**, 635 (1993).
[27] M. S. Chowdhury, W. Booth, and R. N. Glover, IL Nuovo Cimento **99**, 701 (1988).
[28] E. R. Flynn, F. Ajzenberg-Selove, R. E. Brown, J. A. Cizewski, and J. W. Sunier, Phys. Rev. C **24**, 2475 (1981).
[29] R. A. Meyer, E. A. Henry, L. G. Mann, and K. Heyde, Phys. Lett. **B177**, 271 (1986).
[30] Alan B. Smith, J. Phys. G: Nucl. Part. Phys. **26**, 1467 (2000).
[31] E. R. Flynn, F. Ajzenberg-Selove, R. E. Brown, J. A. Cizewski, and J. W. Sunier, Phys. Rev. C **24**, 902 (1981).
[32] G. Kajrys, S. Landsberger, R. Lecomte, P. Paradis, and S. Monaro, Phys. Rev. C **26**, 1451 (1982).